The Environmental *Acinetobacter baumannii* Isolate DSM30011 Reveals Clues into the Preantibiotic Era Genome Diversity, Virulence Potential, and Niche Range of a Predominant Nosocomial Pathogen

Guillermo D. Repizo[1,2,*], Alejandro M. Viale[2], Vítor Borges[3], María M. Cameranesi[2], Najwa Taib[4], Martín Espariz[2], Céline Brochier-Armanet[4], João Paulo Gomes[3], and Suzana P. Salcedo[1]

[1]Laboratory of Molecular Microbiology and Structural Biochemistry, CNRS UMR5086, University of Lyon, France

[2]Departamento de Microbiologia, Instituto de Biologia Molecular y Celular de Rosario (IBR, CONICET), Facultad de Ciencias Bioquimicas y Farmaceuticas, Universidad Nacional de Rosario, Argentina

[3]Bioinformatics Unit, Department of Infectious Diseases, National Institute of Health, Lisbon, Portugal

[4]Laboratoire de Biométrie et Biologie Évolutive, Univ. Lyon, Université Lyon 1, CNRS, UMR5558, Villeurbanne, France

*Corresponding author: E-mail: repizo@ibr-conicet.gov.ar.

Accepted: August 24, 2017

Data deposition: The whole genome shotgun project for A. baumannii DSM30011 has been deposited at DDBJ/ENA/GenBank under the accession JJOC00000000. The version described in this paper is version JJOC02000000.

Abstract

Acinetobacter baumannii represents nowadays an important nosocomial opportunistic pathogen whose reservoirs outside the clinical setting are obscure. Here, we traced the origins of the collection strain *A. baumannii* DSM30011 to an isolate first reported in 1944, obtained from the enriched microbiota responsible of the aerobic decomposition of the resinous desert shrub guayule. Whole-genome sequencing and phylogenetic analysis based on core genes confirmed DSM30011 affiliation to *A. baumannii*. Comparative studies with 32 complete *A. baumannii* genomes revealed the presence of 12 unique accessory chromosomal regions in DSM30011 including five encompassing phage-related genes, five containing toxin genes of the type-6 secretion system, and one with an atypical CRISPRs/cas cluster. No antimicrobial resistance islands were identified in DSM30011 agreeing with a general antimicrobial susceptibility phenotype including folate synthesis inhibitors. The marginal ampicillin resistance of DSM30011 most likely derived from chromosomal ADC-type *ampC* and bla_{OXA-51}-type genes. Searching for catabolic pathways genes revealed several clusters involved in the degradation of plant defenses including woody tissues and a previously unreported *atu* locus responsible of aliphatic terpenes degradation, thus suggesting that resinous plants may provide an effective niche for this organism. DSM30011 also harbored most genes and regulatory mechanisms linked to persistence and virulence in pathogenic *Acinetobacter* species. This strain thus revealed important clues into the genomic diversity, virulence potential, and niche ranges of the preantibiotic era *A. baumannii* population, and may provide an useful tool for our understanding of the processes that led to the recent evolution of this species toward an opportunistic pathogen of humans.

Key words: comparative genomics, preantibiotic era bacterium, virulence factors, CRISPRs/cas.

Introduction

The genus *Acinetobacter*, family *Moraxellaceae*, class *Gammaproteobacteria*, is characterized by Gram-negative aerobic coccobacilli of ubiquitous environmental distribution and large metabolic capabilities (Bouvet and Grimont 1986). Among the genus, the phylogenetically closely-related species composing the *Acinetobacter calcoaceticus–Acinetobacter baumannii* (Acb) complex represent nowadays important opportunistic pathogens (Antunes et al. 2014). Infections due to *A. baumannii* in particular, rarely reported in healthcare

settings before the 1970s, rapidly increased in importance with the global spread of a limited number of epidemic clonal complexes (CC) possessing multidrug-resistance (MDR) phenotypes (Diancourt et al. 2010; Antunes et al. 2014). Strains composing the CCs generally contain plasmids and chromosomally-located resistance islands (RI) and genomic islands (GI) encompassing different transposons and integrons which play pivotal roles in both antimicrobial and heavy metal resistance (Di Nocera et al. 2011; Nigro et al. 2011; Antunes et al. 2014; Touchon et al. 2014). Also, CC strains carry a large repertoire of insertion sequences (ISs) capable of mediating genome rearrangements, deletions, insertions, inversions, and gene overexpression with strong adaptive significances (Roca et al. 2012; Antunes et al. 2014; Touchon et al. 2014). The combination of the above factors, added to the intrinsic resistance of *A. baumannii* to desiccation and fever-associated temperatures, are considered main factors of persistence of pathogenic strains in the nosocomial environment (Roca et al. 2012; Antunes et al. 2014).

Whole-genome sequence (WGS) comparisons have become commonplace in examining strain-to-strain variability and in comparing pathogenic strains with environmental, less aggressive relatives in efforts to identify underlying genetic determinants and mechanisms responsible for phenotypic dissimilarities. When applied to *A. baumannii*, these approaches provided valuable information on both the present *A. baumannii* population structure and the mechanisms of acquisition and evolution of antimicrobial resistance (Di Nocera et al. 2011, Roca et al. 2012; Antunes et al. 2014; Touchon et al. 2014). It is now generally accepted that *A. baumannii* arose from other members of the Acb complex as the result of an ancient population bottleneck, followed by a recent population expansion from a few clinically-relevant clones endowed with a diverse arsenal of resistance genes (Diancourt et al. 2010; Antunes et al. 2014; Touchon et al. 2014). Still, the identification of *A. baumannii* virulence traits has remained elusive, and in fact large genetic variations have been found both between and within CC members suggesting a complex and even a multifactorial nature of mechanisms involved (Diancourt et al. 2010; Roca et al. 2012; Antunes et al. 2014). In this context it has recently been emphasized the importance of a deeper genomic study of non-clinical ("environmental") isolates to clarify both the virulence potential of the aboriginal *A. baumannii* population and the evolutionary paths that led toward an opportunistic pathogen lifestyle (Antunes et al. 2014). However, and contrasting with the environmental ubiquity of most other members of the genus, the natural habitats and infection reservoirs of *A. baumannii* outside the clinical setting are still to be defined (Eveillard et al. 2013; Antunes et al. 2014). Although *A. baumannii* isolates have been obtained from non-clinical sources including domestic animals, human ectoparasites, vegetables, the plant rhizosphere, etc., whether they represent true environmental isolates or consequences of human waste contamination remains debated (Eveillard et al. 2013; Antunes et al. 2014).

Acinetobacter baumannii DSM30011 is a collection strain amenable for genetic manipulation (Wilharm et al. 2013). This organism is capable of killing *Galleria mellonella* larvae, outcompeting other clinically-relevant bacterial species in a type-6 secretion system (T6SS)-dependent manner, and forming biofilms and biopellicles (Repizo et al. 2015), that is, traits generally associated to bacterial persistence in different environments including the clinical setting (Roca et al. 2012; Longo et al. 2014; Nait Chabane et al. 2014). Here, we traced DSM30011 origins to a strain originally deposited at the NRRL in 1943 as *Achromobacter lacticum* 4-h (NRRL B-551, Agricultural Research Service Culture Collection, ARS, U.S. Department of Agriculture; see supplementary table S1, Supplementary Material online for details). This strain was isolated after enrichment of the resin-degrading natural microbiota responsible of the aerobic decomposition of guayule (*Parthenium argentatum* Gray), a resin-producing angiosperm of the *Asteraceae* family common to arid and semiarid areas of the south-western United States and north-central Mexico (Allen et al. 1944; Naghski et al. 1944). DSM30011 thus provided us with an environmental *A. baumannii* strain isolated by the middle of last century just before the onset of the antibiotic era (Antunes et al. 2014), and therefore well-differentiated both temporally and epidemiologically from the clinical strains predominant nowadays. Here, we conducted a comparative genomic analysis of DSM30011 with other *Acinetobacter* strains to obtain clues into the genomic diversity and virulence potential of the preantibiotic era *A. baumannii* population.

Materials and Methods

Strain Sources

The DSM30011 strain used for genome sequencing in this work was obtained from the DSMZ-German Collection of Microorganisms and Cell Cultures (Braunschweig, Germany), and was kindly provided to us by Dr X. Charpentier (CIRI, Lyon, France). The original isolation and different denominations assigned to this strain by various collections are detailed below, under "Tracing DSM30011 origins" and in supplementary table S1, Supplementary Material online. *Acinetobacter* sp. strains NCIMB8208 and NCIMB8209 were obtained from the National Collection of Industrial Food and Marine Bacteria (NCIMB, Aberdeen, Scotland). The *A. baumannii* type strains ATCC19606 and ATCC17978 were part of the laboratory stock collection.

Genotypic Analysis

The evaluation of genomic differences between the different strains was done by a random amplification of polymorphic DNA assay using as primers the degenerate oligonucleotides

5′-GGTCGACYNGGRTC-3′ (#5314) and 5′-GGTCGACYT TNGYNGGRTC-3′ (#19) (Limansky and Viale 2002).

DSM30011 Genome Sequencing and Annotation

DSM30011 DNA was isolated using the DNeasy Blood and Tissue kit (Qiagen) following the manufacturer's protocols. The genomic sequence was obtained using a paired-end (2 × 250 bp) strategy using the Illumina MiSeq method and following the protocols provided by the supplier. A total of 3,581, 922 × 2 reads were generated with an average length of 250 bp. Reads were subjected to quality assessment and further assembled using the Velvet version 1.2.10 (k-mer size used was 97). The de novo assembly process was optimized using the VelvetOptimiser script version 2.2.5. The resulting contigs were ordered and oriented with Mauve (Darling et al. 2010) using the *A. baumannii* ATCC17978 genome as reference. When necessary, the contigs were concatenated by including the sequence nnnnncacacacttaattaattaagtgtgt gnnnnn, that harbors stop codons in all six reading frames as was described in Repizo et al. (2014). The replication origin (*oriC*) was predicted by OriFinder (Gao and Zhang 2008). Assembled genome sequences were annotated using RAST (Aziz et al. 2008). Coding sequences (CDS) functions were manually curated using BLASTP searches (*e* value $= 1 \times e^{-10}$) of the NCBI nonredundant database. This whole genome shotgun project has been deposited at DDBJ/ENA/GenBank under the accession JJOC00000000. The version described in this paper is version JJOC02000000.

The presence of mobile genetic elements in the DSM30011 genome was investigated by the following online tools and/or open-access database and manual examinations: IslandViewer (http://pathogenomics.sfu.ca/islandviewer; Dhillon et al. 2015) for the GI regions and IS Finder (Siguier et al. 2006; https://www-is.biotoul.fr/) and ISSaga (Varani et al. 2011) for IS elements. CRISPRs were detected using the CRISPRs recognition tool v1.1 (Bland et al 2007), whereas putative prophage sequences were identified by PHAST and PHASTER analysis (Zhou et al. 2011; Arndt et al. 2016). Genes encoding antibiotic resistance were identified with ResFinder 2.1 (https://cge.cbs.dtu.dk/services/ResFinder/; Zankari et al. 2012) and RAST.

Phylogenetic and Shared Protein Families Analyses

To infer the relationships among the 64 *Acinetobacter* strains analyzed in this work which included 32 *A. baumannii* strains other than DSM30011, the corresponding proteomes were first retrieved from the NCBI and gathered into a local database together with the DSM30011 proteome. Homologous protein families were assembled with SILIX version 1.2.9 (Miele et al. 2011). More precisely, pairwise comparisons of proteins contained in the local database were performed using the BLASTP program version 2.2.26 with default parameters (Altschul et al. 1997). Proteins in a pair providing HSP (High-scoring Segment Pairs) with identity over 80% and covering at least 80% of the protein lengths were gathered together in the same family. This led to the assembly of 42,211 families. Association coefficients (S_{AB}) were computed for each pair of strains as $S_{AB} = (100 \times 2N_{AB})/(N_A + N_B)$, in which N_A is the number of protein families present in strain A, N_B is the number of protein families present in strain B and N_{AB} is the number of protein families shared by strain A and strain B. This coefficient ranged from 0 when both strains do not share any gene family to 1 when all the families present in strain A were also present in strain B.

Among the 42,211 inferred protein families, 351 correspond to core gene families present in a single copy in all 64 *Acinetobacter* strains. For each family, the corresponding nucleotidic sequences were aligned with MUSCLE 3.8.31 (default parameters) on the basis of the aligned protein sequences, so as to preserve the codon integrity by avoiding introduction of incorrect frame shifts. The resulting 351 multiple alignments were then trimmed using BMGE1.1 with the CODON option (Criscuolo and Gribaldo 2010) and combined to build a large supermatrix (385, 926 nucleotide positions) that was used for phylogenetic inferences. A phylogenetic tree was then inferred with the Maximum Likelihood (ML) approach using IQTREE (Nguyen et al. 2015) with the GTR + R6 evolutionary model. The branch robustness of the ML tree was estimated with the nonparametric bootstrap procedure implemented in IQTREE (100 replicates of the original alignment).

Sequence Typing

Assignment of sequence types (ST) for DSM30011 was done using housekeeping genes: *cpn60*, *gdh*, *gltA*, *gpi*, *gyrB*, *recA*, and *rpoD* (Oxford scheme, Bartual et al. 2005) or *cpn60*, *fusA*, *gltA*, *pyrG*, *recA*, *rplB*, and *rpoD* (Pasteur scheme, Diancourt et al. 2010). For details see supplementary table S2, Supplementary Material online and the *A. baumannii* MLST Databases website (http://pubmlst.org/abaumannii/; Jolley and Maiden 2010).

Antimicrobial Susceptibility Testing

The general antimicrobial susceptibility of *A. baumannii* strains DSM30011, ATCC17978, and ATCC19606 was evaluated using the VITEK 2 System (bioMérieux) following the criteria recommended by the CLSI (Clinical and Laboratory Standards Institute, 2016, Performance standards for antimicrobial susceptibility testing. Document M100S, 26th ed., CLSI, Wayne, PA). Susceptibility tests to tetracycline, chloramphenicol, and macrolides such as azithromycin and erythromycin were done separately by disk assays on Mueller–Hinton agar (MHA) following CLSI protocols. In short, DSM30011 cells were grown overnight at 37 °C, resuspended in LB broth to a turbidity of 0.5 McFarland units, and spread on the surface of MHA-containing Petri plates. Antibiotic disks were then carefully

deposited at the center of the agar surface, and the plates were incubated at 37 °C for 16 h before measuring the diameter of the corresponding growth inhibition zones.

Results and Discussion

Tracing DSM30011 Origins

This strain was isolated prior to 1,944 (see supplementary table S1, Supplementary Material online for details) from the natural microbiota enriched during the aerobic decomposition of defoliated guayule plants. This process, known as retting, was applied to reduce the content of terpene resins prior to the extraction of natural rubber for the industrial production of latex (Allen et al. 1944; Naghski et al. 1944). It involved a prior treatment of milled guayule shrubs in boiling water both to remove surface matter and to hydrate/soften the plant tissues, followed by the aerobic decomposition under high moisture of the resulting plant material by the prolific microbiota that survived the above treatment and which was located primarily within the bark (Naghski et al. 1944). This resulted in a marked disintegration of the woody tissues driven by a consortium of different fungal and bacterial groups, from which a number of isolates were isolated with the ability to degrade guayule resins. Among them group III-2b isolates (which fitted at the time the phenotypic description of *A. lacticum*) encompassed non-motile bacterial coccoid rods capable of growing up to 50 °C (Allen et al. 1944). Two of these isolates were deposited in 1943 at the Agricultural Research Service Culture Collection (ARS, NRRL, USDA) under the denominations *A. lacticum* B-551 and B-552, respectively, and were subsequently replicated in other collections under other designations including *Acinetobacter* sp. strains NCIMB8208 and NCIMB8209, respectively (see supplementary table S1, Supplementary Material online for details). A more comprehensive phenotypic analysis later conducted on these strains reassigned them to the newly described genus *Acinetobacter* Brisou and Prévot (Thornley 1967). More recently, and on the basis of *rpoB* sequence comparisons, the B-551 replica present at the Culture Collection of the Institute Pasteur (CIP68.38) was assigned to *A. baumannii* as a species (La Scola et al. 2006; Gundi et al. 2009). The phylogenetic analysis conducted here using core genes sequence comparisons (see below) allowed us to validate this assignment for the equivalent replica (DSM30011) present at the German Collection of Microorganisms and Cell Cultures (DSMZ, Braunschweig, Germany). We also verified the genomic identity between *A. baumannii* DSM30011 and NCIMB8208 by a random amplification PCR assay (supplementary fig. S1*A*, Supplementary Material online), which showed identical amplification profiles as expected from strains derived from the same isolate (Limansky and Viale 2002). In turn, the above profiles could be clearly differentiated from those obtained for other strains isolated during a similar time period including the clinical *A. baumannii* strains ATCC19606 and ATCC17978, and even from the companion strain NCIMB8209 (supplementary fig. S1*A* and table S1, Supplementary Material online), therefore indicating that they belong to different clonal lineages. It is also worth noting that DSM30011/NCIMB8208 can grow at 44 °C (supplementary fig. S1*B*, Supplementary Material online) in what represents a typical phenotype associated to *A. baumannii* but not to other *Acinetobacter* members (Bouvet and Grimont 1986; Nemec et al. 2011).

DSM30011 thus provided us with an *A. baumannii* strain originally isolated in the USA from a resinous desert plant >70 years ago, that is, on the verge of the massive introduction of antibiotic therapy to treat infections (Allen et al. 1944). Also, isolation of this strain preceded by a few years those of the *A. baumannii* clinical strains ATCC19606 (USA, 1948) and ATCC17978 (France, 1951; supplementary table S1, Supplementary Material online).

Genomic Features

DSM30011 genome sequencing (depth of coverage ~350×) resulted in 13 contigs ranging from 309 to 1,346,914 bp in length, with an average size of 247,059 bp. The draft genome thus encompassed 3,949,168 bp with a G + C content of 38.7% (table 1), values that matched the averages reported for the genomes of the species composing the *Acinetobacter* genus (3.87 Mb and 39.6% respectively; Touchon et al. 2014). A total of 3,774 CDS and 62 structural RNAs (60 tRNAs and 2 rRNAs regions), were predicted by RAST (Aziz et al. 2008) in DSM30011 (table 1). The annotation covered 448 RAST subsystems (47%) with 1,746 CDS; 64 CDS being labeled as hypothetical proteins. On the other hand, 2,028 CDS (53%), from which 1,045 corresponded to hypothetical proteins, could not be assigned to any subsystem. No DNA sequences matching plasmid sequences deposited in GenBank were found, and no plasmids could be detected in DSM30011 using ordinary plasmid-extraction protocols (not shown).

Phylogenetic and MLST Analyses

ML phylogenetic analysis based on the comparisons of the concatenated sequences of 351 core genes of 64 different *Acinetobacter* strains including species of the Acb complex (listed in supplementary table S3, Supplementary Material online) indicated a clear affiliation (bootstrap value (BV) = 100%) of DSM30011 to the *A. baumannii* cluster (fig. 1 and supplementary fig. S2, Supplementary Material online). Among this cluster, and with some exceptions such as the distinct subgroups formed by each the CCI and CCII strains, the relationships among *A. baumannii* strains (including DSM30011) were not well-resolved (most BV < 50%, fig. 1*A*). These observations agree with the lack of phylogenetic structure reported for the *A. baumannii* population (Diancourt et al. 2010). These authors found no evidence of

phylogenetic structure within the clinical *A. baumannii* strain population analyzed, with the exception of a few tight terminal clusters corresponding to CCs of much more recent emergence (post1950) connected to the introduction of massive antimicrobial therapy.

A. baumannii DSM30011 was assigned to novel sequence types on both MLST classification schemes currently in use: ST 1113 in the Oxford scheme and ST 738 in the Pasteur scheme (see supplementary table S2, Supplementary Material online). The fact that DSM30011 shared only 3 of 7 alleles (Oxford scheme) or 4 of 7 alleles (Pasteur scheme) with any closest matching strain (supplementary table S2, Supplementary Material online) prevented us to relate this strain to any of the different CC or ST presently defined (Karah et al. 2012).

Table 1

General Features of the DSM30011 Genome[a]

Feature	Value
Estimated size (Mbp)	3.95
GC content (%)	38.7
Number of CDSs	3,774
CDSs with predicted function (%)	70.6
Conserved hypothetical CDSs (%)	29.4
Number of tRNA genes	60
Number of rRNA operons	2
Phage regions	5
Complete ISs[b]	0
CRISPRs-cas clusters	1

[a]On the basis of RAST annotation.

[b]IS1236-like and ISAba8-like remnants were detected (see supplementary table S7, Supplementary Material online).

Comparative Genomics of DSM30011

As indicated above, DSM30011 represents the earliest *A. baumannii* isolate reported to-date obtained from a non-clinical source. We therefore conducted a comparative genomic analysis of this strain in an effort to obtain clues on the diversity of the *A. baumannii* population existing before the antibiotic era (Antunes et al. 2014). We compared the proteomes of 64 *Acinetobacter* including the strain DSM30011 and 32 *A. baumannii* which allowed us to assemble 42,211 protein families. Regarding DSM30011 (3,774 predicted CDS), 3,725 families contain at least one sequence from this strain, and among these, 1.3% included >1. While 243 protein families were specific to DSM30011, 1,935 (51.9%) were shared by all *A. baumannii* strains. This number was close to recent estimations of the core genome content of this species (Peleg et al. 2012, Touchon et al. 2014). When core plus accessory genomes were compared, DSM30011 shared the highest number of CDSs (3,157 protein families, supplementary fig. S3, Supplementary Material online) with *A. baumannii* IOMTU-433, a MDR clinical strain recently isolated from a patient in Nepal (BioSample: SAMD00020223). On the other hand, DSM30011 shared the lowest number of CDSs with NCGM-237 (2,769 protein families), a MDR-strain isolated

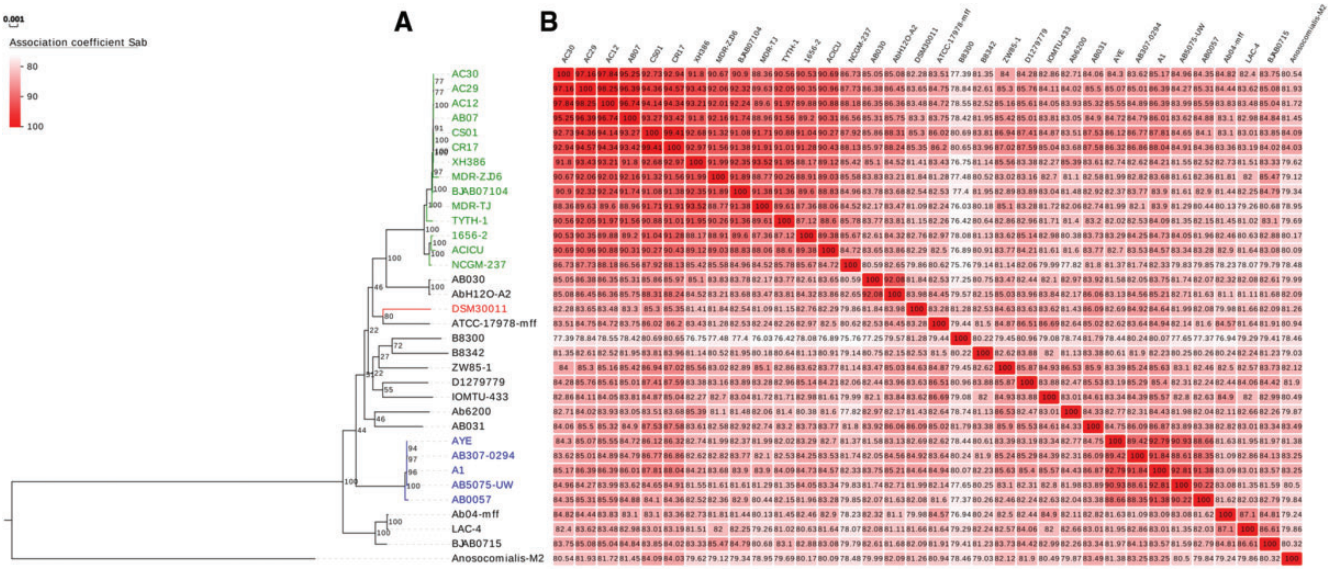

Fig. 1.—Maximum Likelihood phylogenetic analysis of *Acinetobacter baumannii* strains accompanied by the association coefficient for each pair of strains. (*A*) The ML phylogeny was computed based on 351 concatenated core gene sequences (full tree is shown in supplementary fig. S2, Supplementary Material online). Numbers at nodes correspond to bootstrap values (100 replicates of the original data set). The scale bar below corresponds to evolutionary distance (average number of the substitutions per site). CCI (in blue) and CCII (in green) correspond to subclusters formed by *A. baumannii* species assigned to epidemic clonal complexes CCI and CCII, respectively. (*B*) The table corresponds to the S_{AB} association coefficient computed for each pair of strains as twice the number of shared gene families between the two strains divided by the number of gene families contained in the two strains, considering all the gene families (see Methods for details).

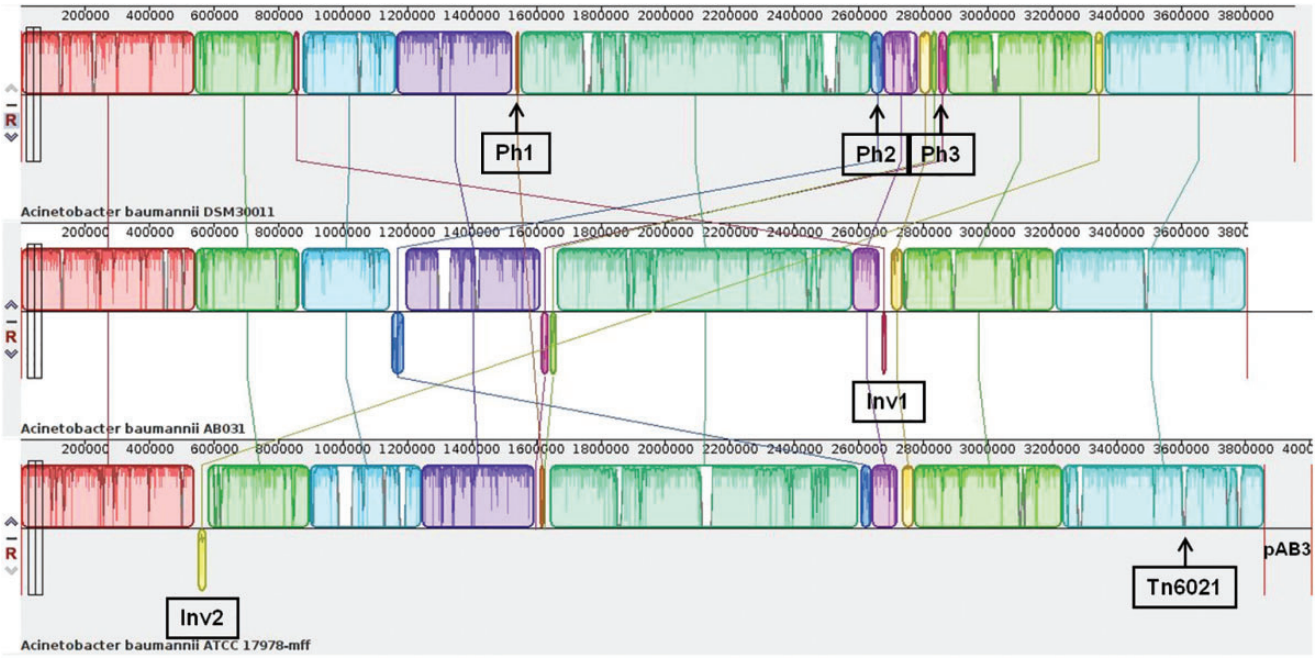

Fig. 2.—Linear comparison of the genomes of *A. baumannii* strains DSM30011, AB031, and ATCC17978 inferred using Mauve. Each block corresponds to a DNA fragment of the chromosome distinctively colored for clarity. The degree of conservation is indicated by the vertical bars inside the blocks. Their position relative to the genome line denotes colinear and inverted regions. Putative prophage insertions (Ph1-3) are indicated below the DSM30011 genome (see supplementary table S6, Supplementary Material online for details). DNA inversions (Inv1-2) and the insertion of Tn6021 within *comM* in ATCC17978 are also shown (see text for details).

in Japan (Tada et al. 2014). However, these values could be biased by differences in strain proteome size. Indeed, based on association coefficients (S_{AB}, see Methods), DSM30011 appeared more similar in terms of shared gene families to AB031 ($S_{AB} = 86.09$, Fig. 1B), a tigecycline- and sulfamethoxazole/trimethoprim-resistant clinical isolate obtained from a bloodstream infection in Canada (Loewen et al. 2014). In addition, based on the same criterion DSM30011 was less similar to NCGM-237 ($S_{AB} = 79.86$). Intermediate values were obtained for ATCC17978 ($S_{AB} = 83.28$; 3,055 shared protein families), a clinical strain almost contemporary to DSM30011 (supplementary table S1, Supplementary Material online) which emerged in close proximity in the core genes phylogenetic tree of figure 1*A* (BV: 82%).

The genomes of strains AB031 and ATCC17978 were individually used as scaffolds to organize the contigs obtained for DSM30011 (fig. 2). Since a lower number of block rearrangements were required to organize the DSM30011 genome when ATCC17978 was used as reference, we adopted the genomic organization based on the latter strain for further analyses.

The inferred organization of the DSM30011 genome was compared with the whole genomes (chromosome and plasmids) of the two aforementioned *A. baumannii* strains. As seen in figure 2, a general shared synteny resulted between all of these genomes except for some worth-noting differences such as: 1) the presence, position and orientation of a 17 kbp-segment (Inv1) encompassing a GI conferring resistance to heavy metals (see also the immediate section below). This GI, which is notoriously missing in strain ATCC17978, is located in a different genomic locus and also in an inverted position in strain AB031 as compared with DSM30011; 2) several regions harboring putative prophages (Ph1-3) that will be described in detail below; 3) the presence, position, and orientation of a 33 kbp-segment (Inv2) encompassing a GI conferring resistance to heavy metals (see DSM30011 antimicrobial resistance). This GI is located in a different genomic locus and in an inverted position in strain ATCC17978 and is notoriously missing in strain AB031; 4) the interruption of the *comM* gene by Tn6021 in strain ATCC17978.

Two hundred and forty three proteins of the DSM30011 predicted proteome belong to protein families containing only DSM30011 CDS according to the parameters used to build the protein families with SILIX (see Methods). Subsequent BLAST sequence similarity-based comparison (*e* value cut-off $1 \times e^{-4}$) of these 243 sequences against our local database (64 acinetobacter proteomes) revealed that 83 sequences have a hit in at least one other *A. baumannii* strain. Those sequences represent likely divergent homologues that could not be affiliated to any gene family because they did not fit the parameters used for protein family delineation by SILIX. one hundred thirty eight CDS (*e* value $> 1 \times e^{-4}$) presented

no significant hits (false positives), and 22 CDS had no hits. Blasting the 243 CDS against a larger database containing >5,000 complete genomes from *Archaea* and major bacterial phyla (including 43 *A. baumannii* proteomes) revealed 89 CDS with significant best hits in *A. baumannii*; 52 CDS were affiliated with other gammaproteobacteria, 20 with other bacterial phyla, 69 (*e* value $> 1 \times e^{-4}$) provided no significant hits (false positives) and 13 showed no hits at all (supplementary table S4, Supplementary Material online). Among this group of 243 CDS, we distinguished 12 accessory gene clusters (AGC I–XII; table 2 and fig. 3*A*) from which eight were predicted as horizontally-transferred GIs (supplementary table S5, Supplementary Material online). Five AGCs (III, V, VI, VIII, and X), encompassed phage-related genes (table 2). In this regard, one incomplete and two intact prophages (supplementary table S6, Supplementary Material online) were identified in these DNA regions. All prophages shared significant sequence identities with the podoviral lytic bacteriophage YMC/09/02/B1251 ABA BP (NC_019541.1; Jeon et al. 2012). The intact prophages were 46.0 and 50.7 kbp long, contained a G + C of 39.2% and 37.9%, respectively, and harbored 66 and 69, respectively, open reading frames. Putative *attL* and *attR* recombination sites were detected in each case (supplementary table S6, Supplementary Material online).

Interestingly, homologs of the error-prone DNA polymerase V subunits *umuC* (DSM30011_07275 and DSM30011_13575) and *umuD* (DSM30011_13570) were associated to or located within prophage regions 1 and 3 respectively (supplementary table S6, Supplementary Material online), a situation similar to that described for *A. baumannii* ATCC17978 (Hare et al. 2014). Furthermore, another *umuD* paralogue (DSM30011_10830) and genes encoding error-prone polymerases such as DinP (DSM30011_17910) and DnaE2 (DSM30011_10470; Norton et al. 2013) were found in the DSM30011 genome. The high frequency in *Acinetobacter* members of genes encoding these polymerases has already been noticed previously (Touchon et al. 2014), and proposed to play roles in the diversification of the genus including the mutational acquisition of resistance to toxins and antimicrobials.

RloC tRNAses have been proposed to be involved in resistance to phages (Davidov and Kaufmann 2008). A *rloC* homolog gene (DSM30011_00955) was identified next to AGC II (supplementary table S4, Supplementary Material online) in a region predicted to be part of GI 2 (supplementary table S5, Supplementary Material online) also present in *A. baumannii* ATCC19606.

AGCs I, IX, and XII encompass loci encoding T6SS-related VgrG proteins and associated antibacterial effectors (Repizo et al. 2015). Two additional gene clusters coding for putative T6SS-toxins (AGCs VII and XI) and cognate immunity proteins were also revealed by our analysis (supplementary table S4, Supplementary Material online). The diverse arsenal of T6SS-associated toxin genes encoded within GIs (supplementary table S5, Supplementary Material online) may possess adaptive significance, especially to compete with other microbes of the environment (Repizo et al. 2015).

A Mobile Elements Faulty Genome

Notably, and in sharp contrast to clinical *A. baumannii* strains (Peleg et al. 2012; Roca et al. 2012; Antunes et al. 2014; Touchon et al. 2014), an extremely low representation of transposable genetic elements such as IS or transposons was found in the DSM30011 genome. Nevertheless, defective versions of mobile genetic elements were found next to AGC III (supplementary tables S4 and S7, Supplementary Material online). In this region, we detected remnants of an IS1236/ISAcsp3 element (fig. 3*B*) of the IS3 family typical of the soil species *Acinetobacter baylyi* ADP1 (Gerischer and Ornston 1995), whose *tnpA* gene had been disrupted by an ISAba8-like element from which we located only the complete left inverted repeat (IR-L) and a short internal fragment of 41 bp (fig. 3*B* and supplementary fig. S4, Supplementary Material online). The latter fragment was preceded by the 3′ end of the *hsdR* gene belonging to a *hsdMRS* operon encoding a tripartite Type I restriction-modification (TIM) system and by two *fic* genes encoding a toxin–antitoxin (TA) system (fig. 3*B*). The association of TA and TIM systems in bacterial chromosomes in so-called defense islands (DI) against incoming DNA from viruses and plasmids has been previously reported, and their maintenance explained due to the deleterious effects resulting from the loss of the addictive elements that compose these systems (Makarova et al. 2011). Some DI are in turn associated to either active or inactivated mobile elements (Makarova et al. 2011), which seems the case for DSM30011. As seen in figure 3*B*, the TIM/TA arrangement is in turn preceded by a previously unreported Tn6018 variant (Tn6018-like) showing complete IR-L and IR-R repeats, but whose *tnpA* gene is interrupted by a *merR-merTPCAD* gene cluster coding for a complete Hg ion detoxification system (Boyd and Barkay, 2012). As seen in this figure this Tn6018 additionally carried *cad* genes encoding a Co/Zn/Cd ions tolerance system (Post et al. 2010). Tn6018 transposons are generally embedded within AbaR RI in clinical *A. baumannii* strains (Post et al. 2010), but this is clearly not the case of DSM30011 as discussed above. The particular assembly of metal detoxification systems in this Tn6018 variant may have provided DSM30011 cells with additional efflux capacity for different heavy metal ions, and represented an early stage in the formation of a RI toward toxic compounds increasingly found in the environment. Our search for similar assemblies in *Acinetobacter* genomes detected similar Tn6018 arrangements in the *A. baumannii* strains AB031, ATCC19606, 121738, 466760, MSP4-16 and in *Acinetobacter* sp. CIP 53.82.

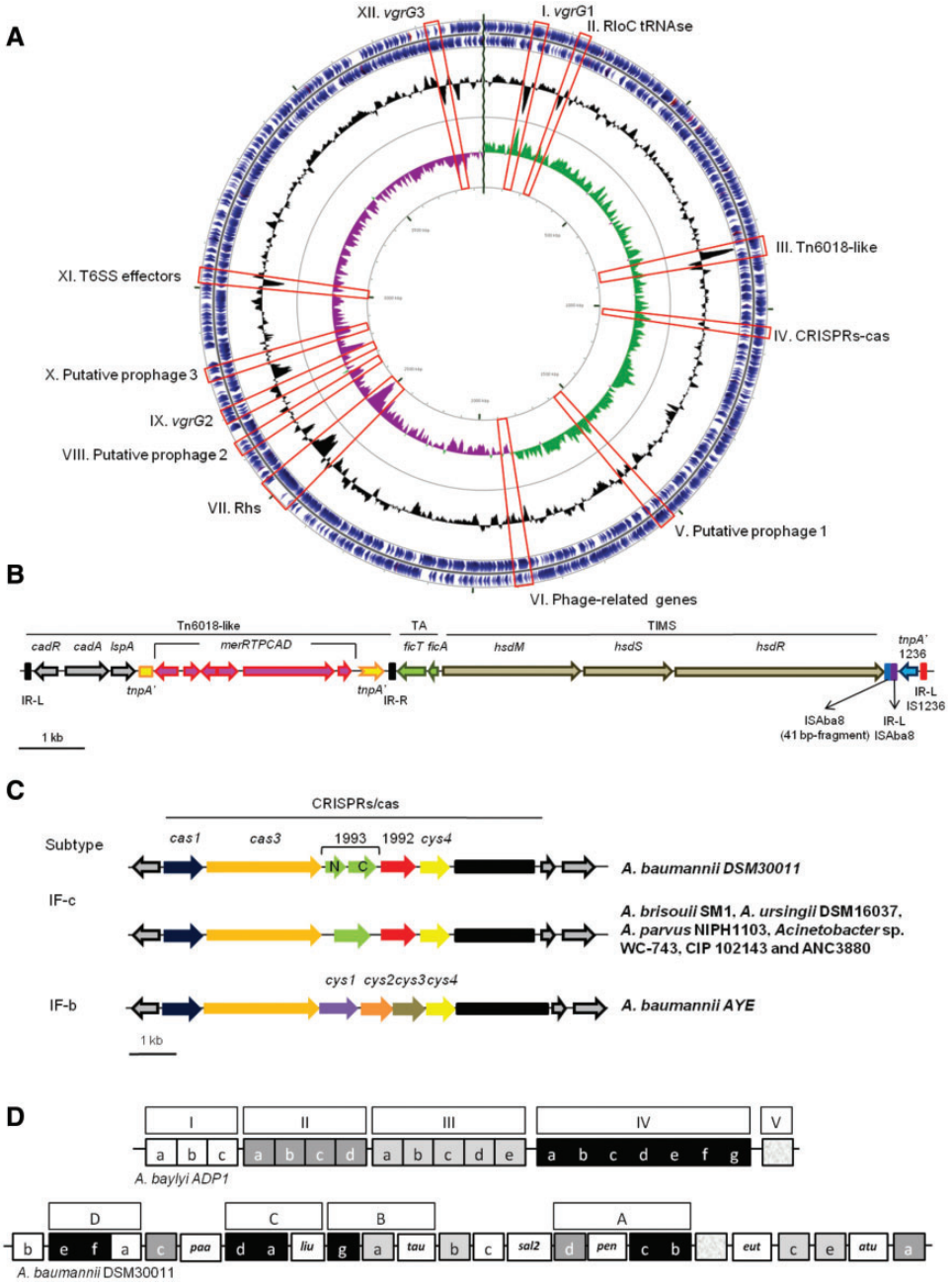

Fig. 3.—Genomic features of *A. baumannii* DMS30011. (*A*) Genome map. The two outermost circles denote the positions of protein (blue) and RNA (red) coding sequences on the plus (circle 1) and minus (circle 2) strands. Circle 3 (black) indicates the GC content. Circle 4 denotes positive (green) and negative (purple) GC-skew. The different accessory gene clusters (AGC I–XII) characteristic of DSM30011 (see table 2 for details) are indicated by red boxes. The CGView software (Stothard and Wishart 2005) was used to construct the genome map. (*B*) Schematic representation of the genomic region encompassing Tn6018-like region and IS1236/ISAcsp3 mobile elements. (*C*) Schematic representation of the CRISPR-*cas* cluster. This locus (designated as subtype IF-c) is compared against a group of *Acinetobacter* strains bearing a locus with a similar genetic organization and also against *A. baumannii* AYE, the reference strain for the subtype IF-b. (*D*) Content and organization of catabolic loci in DSM30011 as compared with *A. baylyi* (Barbe et al. 2004). This figure follows and complements the schematical representation of catabolic loci elaborated by Di Nocera et al. (2011; see fig. 4 therein). Equivalent catabolic loci between the two strains are indicated by similar shades, and those present only in DSM30011 (*liu*, *tau*, *pen*, and *atu*) are indicated by open boxes. The composition of catabolic islands *A*–*D* in DSM30011 is indicated.

Table 2
Accessory Gene Clusters (AGC) Specific of DSM30011 as Compared with Other *A. baumannii* Genomes

AGC[a]	GI[b]	Locus Tag (DSM30011_)	Locus Description
I	1	00495–00510	*vgrG*-associated region 1
II	2	00930–00940	RloC-dependent phage defensive mechanism
III	4	04065–04170	Phage-related genes located next to Tn6018-like element
IV	–	04925–04935	CRISPRs-cas cluster
V	–	07035–07240	Putative prophage 1[c]
VI	–	08780–08870	Phage-related genes
VII	7	11710–12025	Region enriched in Rhs family protein-genes
VIII	–	12710–13875	Putative prophage 2[c]
IX	8	13255–13320	*vgrG*-associated region 2
X	9	13765–13660	Putative prophage 3[c]
XI	10	14490–14590	T6SS putative effectors/Type I restriction-modification system
XII	12	18385–18475	*vgrG*-associated region 3

[a]Refer to supplementary table S4, Supplementary Material online.
[b]Refer to supplementary table S5, Supplementary Material online.
[c]Refer to supplementary table S6, Supplementary Material online.

An Atypical CRISPR-*Cas* Cluster in DSM30011

The genomic survey of DSM30011 identified a cluster of genes encoding a CRISPR-*cas* adaptive immune system (Makarova and Koonin 2015) located in AGC IV (supplementary table S8, Supplementary Material online). This *cas* cluster consists of six genes encoding a Cas1 endonuclease, a Cas3/Cas2 helicase/RNAse, a PBPRB1993-like N-terminal region, a PBPRB1993-like C-terminal region, a PBPRB1992-like protein, and a Csy4 protein, respectively (fig. 3C). Downstream of this locus it was found an array of 51 direct repeats of 28 bp, each separated by a 32 bp spacer (supplementary table S8, Supplementary Material online). A comparison between this system and the most common I-Fb CRISPR-*cas* subtype reported for *A. baumannii* (Touchon et al. 2014; Karah et al. 2015) indicated several differences (fig. 3C). The DSM30011 system could be assigned to the subtype I-F variant 2 of the classification of Makarova and Koonin (2015), in which PBPRB1992 and PBPRB1993 are in fact associated canonical proteins. A search for similar CRISPR-*cas* clusters identified analogous arrangements in two other *A. baumannii* strains: 869535 and 507_ABAU, in other *Acinetobacter* species such as *Acinetobacter brisouii* SM1, *Acinetobacter ursingii* DSM16037, and *Acinetobacter parvus* NIPH1103; and in *Acinetobacter* sp. isolates including WC-743, CIP 102143, and ANC3880 (fig. 3C and supplementary table S8, Supplementary Material online). Therefore, the CRISPR-*cas* cluster identified in DSM30011 and the above *Acinetobacter* strains represented a new subtype, for which we propose the designation I-Fc.

DSM30011 Antimicrobial Resistance

Conventional antimicrobial susceptibility assays indicated that DSM30011 showed clinical susceptibility to most antimicrobials tested except nitrofurantoin and, among β-lactams, ampicillin at MIC values just above CLSI recommended breakpoints (table 3). It is therefore not surprising that this strain lacks all previously characterized AbaR RI (Di Nocera et al. 2011; Roca et al. 2012). The ampicillin resistance of this strain most likely reflects the presence of β-lactamase genes (supplementary table S9, Supplementary Material online) including an *ampC* gene coding for an enzyme sharing 99.2% identity with cephalosporinase ADC-2 (GenBank accession WP_004746565.1) and a bla_{OXA-51}-type gene encoding an enzyme identical to OXA-65 (GenBank accession AAW81337.1, Brown and Amyes 2005). The presence of these two genes in the chromosome of this environmental strain reinforces proposals that both provided for the intrinsic β-lactamase gene repertoire of *A. baumannii* (Turton et al. 2006; Hamouda et al. 2010, Roca et al. 2012; Evans and Amyes 2014).

DSM30011 also contains a *carO* (variant IV) homolog (DSM30011_04565) described only in *A. baumannii* (Mussi et al. 2011) and an *oprD/occAB1* homolog (DSM30011_17845), two genes encoding outer membrane (OM) proteins proposed to participate in the permeation of carbapenems into the periplasm (Morán-Barrio et al. 2017). Resistance to cephalosporins and carbapenems in MDR strains of *A. baumannii* generally results, besides contributions of reduced OM permeability (Mussi et al. 2011; Morán-Barrio et al. 2017), from the overproduction of ADC-type and OXA-type enzymes mediated by IS insertions generating more efficient promoters upstream the corresponding β-lactamase genes (Brown and Amyes 2005; Ravasi et al. 2011; Roca et al. 2012; Evans and Amyes 2014). Although DSM30011 shows susceptibility to both cephalosporins and carbapenems (table 3), it is noteworthy that this strain isolated prior to 1,944 already contained the intrinsic genomic potentiality to evolve such resistances in a highly selective context.

DSM30011 also carries genes potentially providing resistance to aminoglycosides and chloramphenicol including *aacA4*, *aadA*, and *catB2* (supplementary table S9, Supplementary Material online), indicating also a potentiality to evolve such resistances under selective pressure or, alternatively, to serve as reservoir of these resistance genes.

The susceptibility shown by DSM30011 to folate pathway inhibitors such as sulfamethoxazole/trimethoprim (table 3) is worth commenting. The synthetic sulfonamides were introduced for the treatment or prevention of bacterial infections before 1940, and represent the longest employed antimicrobials still in ample use in animal husbandry (Baran et al. 2011). Resistance among bacterial pathogens in the clinical setting emerged and disseminated rapidly after the introduction of sulfonamide therapy, a situation generally driven by mobile

Table 3
DSM30011 Antimicrobial Susceptibility Phenotypes

Method and Antimicrobials Tested			
1) Vitek-2	**MIC (μg/ml)**		
	DSM30011	**ATCC17978**	**ATCC19606**
Ampicillin	16 (R)[a]	16 (R)	≥32 (R)
Cefotaxime	8 (S)	8 (S)	16 (R)
Ceftazidime	4 (S)	4 (S)	16 (I)
Cefepime	2 (S)	≤1 (S)	16 (I)
Imipenem	≤0.25 (S)	≤0.25 (S)	≤0.25 (S)
Meropenem	≤0.25 (S)	≤0.25 (S)	1 (S)
Amikacin	≤2 (S)	≤2 (S)	≤2 (S)
Gentamicin	≤1 (S)	≤1 (S)	8 (I)
Nalidixic acid	≤2 (S)	8 (S)	≤2 (S)
Ciprofloxacin	≤0.25 (S)	≤0.25 (S)	1 (S)
Nitrofurantoin	≥512 (R)	≥512 (R)	256 (R)
Colistin	≤0.5 (S)	≤0.5 (S)	≤0.5 (S)
Sulfamethoxazole/ Trimetoprim (23.75/1.25)	≤20 (S)	160 (R)	≥320 (R)
2) Disk Diffusion[b]	**Diameter Halo (mm)**		
Tetracyclin (30 μg)	23 (S)		
Azithromycin (15 μg)	30 (n.s.[c])		
Erythromycin (15 μg)	27 (n.s.)		
Chloramphenicol (30 μg)	15 (n.s.)		

[a]Susceptibility interpretation (S: susceptible; R: resistant; I: intermediate) according to CLSI standards.
[b]Tested only in DSM30011.
[c]n.s.: not specified in the case of *Acinetobacter* spp., which are considered intrinsically resistant to these antibiotics. In the case of enterobacterial species such as *Salmonella enterica* serovar Typhi a 13 mm zone diameter for azithromycin (15 μg disk) is considered the limit separating susceptible from nonsusceptible isolates, and a 15 mm zone diameter for chloramphenicol (30 μg disk) corresponds to an isolate displaying intermediate resistance to this antibiotic.

genetic elements carrying resistance genes including sulfonamide-resistant forms of dihydropteroate synthase (*sul1*, *sul2*) or different trimethoprim-resistant dihydrofolate reductase (*dfr*; Baran et al. 2011; Nigro and Hall 2011). The susceptibility of DSM30011 to sulfamethoxazole/trimethoprim (table 3) is thus compatible with the absence of *sul* or *dfrA* resistance genes in the genome (this work), and represents a notable exception when compared with clinical strains of *A. baumannii* (Post et al. 2010; Di Nocera et al. 2011; Nigro and Hall 2011; Roca et al. 2012; Loewen et al. 2014; Hamidian and Hall 2016). In this context, the *A. baumannii* clinical strains ATCC19606 and ATCC17978, which were isolated from human clinical samples as early as 1948 and 1951, respectively (supplementary table S1, Supplementary Material online), display sulfamethoxazole/trimethoprim resistance phenotypes (table 3, see also Nigro and Hall 2011; Hamidian and Hall 2016). Sulfonamide resistance in these strains most likely resulted from the lateral acquisition of GI*sul2*-like mobile elements, which were amply distributed among enterobacterial pathogens in the clinical setting worldwide during the first half of last century (Nigro and Hall 2011). The antimicrobial susceptibility shown by DSM30011 (table 3) is thus compatible with an original isolation of this strain in an environment still free of the selection pressure common to the clinical setting at that time.

Genes encoding components of the RND, DMT, MATE, MFS, and SMR efflux systems involved in clinical *Acinetobacter* strains in the extrusion of toxic compounds including some antimicrobials (Roca et al. 2012) were also found in the DSM30011 genome (supplementary table S9, Supplementary Material online). Thus, DSM30011 is also endowed with the capability to evolve reduced susceptibility to at least some of these antimicrobials due to the selection of particular mutations under the context of the corresponding selection pressures.

DSM30011 also contains many gene clusters encoding systems involved in the detoxification of noxious compounds (supplementary table S9, Supplementary Material online). Because all of the above loci are also present in both MDR and drug-susceptible *A. baumannii* strains, we regard them as part of the general detoxification mechanisms intrinsic to this species. In DSM30011 some of these clusters are scattered throughout the genome such as those for Hg and chromate ions (supplementary table S9, Supplementary Material online), while others are concentrated in a region of around 33 kbp constituting a GI (DSM30011_16215 to 16045) integrated next to the *dusA* gene (DSM30011_16220). The latter has been found to represent a common integration site for this kind of genetic elements in *A. baumannii* (Farrugia et al. 2015). This 33 kbp GI includes arsenate and heavy metal ion detoxification systems such as *ars*, *czc*, *cop*, and other genes putatively involved in Fe ions transport (*feoAB*).

Catabolic Potential

WGS analysis identified genes encoding many metabolic pathways involved in the utilization of a large variety of environmental compounds, including many substances produced by plants (supplementary table S10, Supplementary Material online). The presence and organization of different catabolic genes in DSM30011 as compared with the soil bacterium *A. baylyi* (Barbe et al. 2004) are shown in figure 3*D* and supplementary table S10, Supplementary Material online. In *A. baylyi* ADP1 many catabolic loci are clustered in the genome forming five major islands (I–V), which are in turn grouped in a so-called archipelago of catabolic diversity (Barbe et al. 2004). From the 20 loci forming this archipelago in *A. baylyi*, 18 equivalent clusters were detected in DSM30011 (fig. 3*D* and supplementary table S10, Supplementary Material online). Still, some differences were observed in both the organization and even the content of catabolic loci between these two *Acinetobacter* species. These differences included the absence in DSM30011 of loci IIb and IIId encoding the catabolisms of aryl esters and nitriles, a situation also reported for

other *A. baumannii* strains (Di Nocera et al. 2011). In addition, seven other catabolic loci present in DSM30011 were not identified in *A. baylyi* including three (*eut*, *pen*, and *tau*) assigned to the use of ethanolamine, penicillin and taurine, respectively, in other *A. baumannii* strains (Vallenet et al. 2008). Other four catabolic loci also identified in DSM30011 but not in *A. baylyi* were *atu*, *liu*, *sal2/gen*, and *paa* (fig. 3*D* and supplementary table S10, Supplementary Material online). The *atu* locus in particular encodes a complete acyclic terpene degradation pathway (supplementary table S11, Supplementary Material online) homologous to that present in *Pseudomonas aeruginosa* PAO1 (Förster-Fromme et al. 2006). Similarly to *P. aeruginosa*, this pathway is most likely complemented with the *liu* (leucine/isovalerate degradation) cluster (Förster-Fromme et al. 2006) which was identified in DSM30011 in catabolic island C (fig. 3*D*, supplementary tables S10 and S11, Supplementary Material online). It is worth noting that acyclic monoterpenes are major components of isoprenoid oleoresins produced by many plants in response to insects and microbial pathogens (Franceschi et al. 2005; Zulak and Bohlmann 2010). In addition, a search among *Acinetobacter* genomes (supplementary table S3, Supplementary Material online) for this *atu* locus indicated its presence in all Acb complex strains, while on the contrary it was found in only 8 out of 23 non-Acb strains (*Acinetobacter guillouiae* CIP 63.46, *Acinetobacter venetianus* RAG-1 and VE_C3, *Acinetobacter gerneri* DSM 14967, *Acinetobacter beijerinckii* ANC 3835, *Acinetobacter tjernbergiae* DSM 14971, and the *Acinetobacter* sp. isolates ANC4105 and NIPH758).

Further attention was also given to the *dca/pca/qui/pob/hca/van* catabolic loci (Smith et al. 2003), from which the first five are located in island IV of the *A. baylyi* catabolic archipelago and *van* in island Ia (Barbe et al. 2004). The same loci were also located in the DSM30011 genome, but scattered among four different catabolic islands (fig. 3*D* and supplementary table S10, Supplementary Material online). These loci are involved in the degradation of long-chain dicarboxylic fatty acids and hydroxylated aromatic acids including hydroxycinnamic acids, all compounds constituting the hydrophobic heteropolymer suberin (Smith et al. 2003; Barbe et al. 2004). Suberin is located at the outermost layers of plant barks and functions to protect against the attack of insects and pathogens and also to prevent water loss from the tissues below (Franceschi et al. 2005; Graça 2015). The capability of DSM30011 to participate in the breaking down of many plant substances including chemical and physical plant defenses (see above), added to the ability to withstand elevated temperatures (supplementary fig. S1*B*, Supplementary Material online), are compatible with adaptive features selected to thrive in a particularly hostile niche provided by resin-producing desert plants (Allen et al. 1944).

Persistence and Virulence

To analyze the presence of genes potentially involved in persistence and virulence in DSM30011, we first constructed a list of all potential candidates and their regulatory genes (supplementary table S12, Supplementary Material online) described in *Acinetobacter* strains (Roca et al. 2012; Antunes et al. 2014; Eijkelkamp et al. 2014). The list included genes coding for the synthesis of the capsule and other exopolysaccharides, appendages, OM proteins and the T2SS; and also those involved in traits such as motility and iron scavenging. We excluded the superoxide dismutase *sod* gene (Heindorf et al. 2014) and the Tuf elongation factor *tuf* gene (Koenigs et al. 2015) because their ubiquity among the components of the Bacteria realm argues against any specific role of the corresponding gene products in virulence. The genes described in supplementary table S12, Supplementary Material online were thus used as queries to analyze for the presence of orthologs in the DSM30011 genome. As seen in the table 4, most genes encoding proteins with high sequence identity (>90%) to all potential virulence factors analyzed were found in DSM30011.

Among idiosyncratic features of proposed DSM30011 virulence genes worth remarking, we found differences in content and organization of genes linked to the production of K capsule-synthesizing proteins (Hu et al. 2013). The K locus identified in the DSM30011 genome (fig. 4, table 4 and supplementary table S12, Supplementary Material online) displayed a gene organization similar to that previously described for the polysaccharide gene cluster PSgc 20 reported for other *A. baumannii* strains (Hu et al. 2013). Still, the *wagY* glycosyl-transferase gene on the PSgc 20 cluster was found to be replaced by a *wagN* encoding the same function in DSM30011 (fig. 4*A*). Database searching identified the same arrangement in *A. baumannii* strains NIPH 601 and 299505, and in *Acinetobacter* sp. NIPH 1859, therefore indicating a previously unreported PSgc locus common to the above *Acinetobacter* strains.

Furthermore, the gene locus involved in the synthesis of the outer core (OC) of the lipid A core moiety in DSM30011 includes the *rmlBDAC* cluster (supplementary table S12, Supplementary Material online) responsible of the biosynthesis of dTDP-L-rhamnose (fig. 4*B*; Russo et al. 2010, Hu et al. 2013). Rhamnose is a common constituent of *Acinetobacter* surface polysaccharides, and its presence in the OC has been reported to contribute to surface motility in *Acinetobacter nosocomialis* strain M2 (Clemmer et al. 2011).

Another feature worth noting in DSM30011 is the composition of the Bap protein (supplementary fig. S5, Supplementary Material online and table 4). This biofilm-associated OM protein has been shown to participate in biofilm maturation on different abiotic surfaces and in adherence to eukaryotic cells in some *A. baumannii* strains

Table 4
Presence in DSM30011 of Virulence and Environmental Persistence Factors Proposed for *A. baumannii*

Virulence/Persistence Factor	Gene ID (DSM30011_)	Associated Genes	Homologous Loci in Other *Acinetobacter* Members	Reference
EPS	18650–18570	K locus	–	Hu et al. 2013
	02660–02705	OC locus	–	
	01520–01525	O-antigen ligases	M215_10480-75	Harding et al. 2015
	06380–06395	PNAG synthesis I	A1S_2162-60, A1S_3792	Roca et al. 2012;
	14355–14365	PNAG synthesis II	A1S_0940-38	Antunes et al. 2014
Appendages	06115–06140	Csu	A1S_2218-13	Eijkelkamp et al. 2014
	06750–06765	Pilus 2	A1S_2091-88	
	08905–08925	P pilus	AB57_2007-03	
	10220–10235	Pilus 3	A1S_1510-07	
	01445–01465; 01565–01595; 03095–03110; 14670–14675; 17280–17290	T4P	–	Eijkelkamp et al. 2011; Wilharm et al. 2013
	04375/15945	ComEC/ComA	A1S_2610	
Outer membrane proteins	03680–03690	Bap system	ABBFA_RS03900	De Gregorio et al. 2015
	05060	Bap-like	ABBFA_RS05040	
	00870	Omp33	A1S_3297	Roca et al. 2012;
	02970	OmpA	A1S_2840	Antunes et al. 2014
	12485	OmpA like 1	A1S_1193	
	14740	OmpA like 2	A1S_0884	
	13900	Ata	A1S_1033-32	
	18275	Pmt	A1S_0108	
Motility	05005–05010	DAP synthesis	A1S_2454-53	Skiebe et al. 2012
	18220–18255	Biosurfactant synthesis	A1S_0119-12	Clemmer et al. 2011
Iron scavenging	05225–05310	Acinetobactin	ACICU_02570-89	Antunes et al. 2011;
	09010–09020	Fur2-EntBA	ACICU_00267-65	Mortensen and Skaar 2013
	09570–09625	Hydroxamate	ACICU_01683-72	
	09785–09820	Heme	ACICU_01639-32	
	17690–17700	Ferrous ion	ACICU_00267-65	
T2SS[b]	17575–17565; 05860–05865; 15765; 17280; 05690; 17080–17085; 09920–09935		M215_01210-20; 03715-20; 07180; 08525; 08315-20; 14045-14060	Harding et al. 2016
Other factors	08955/02470/02730	Pld1/2/3	HMPREF0010_00607/03706/02731	Stahl et al. 2015
	06960/18680	Plc1/2	HMPREF0010_03297/00294	Fiester et al. 2016
	–	CpaA	M215_05100	Tilley et al. 2014; Harding et al. 2016
	13925	CipA	HMPREF0010_01565	Koenigs et al. 2016

(Roca et al. 2012; Antunes et al. 2014). Bap is composed almost entirely of tandemly arranged amino acid repeats typical of adhesins (bacterial Ig-like 3 domains), and possess a type-1 secretion system target domain probably responsible for its export to the OM. Both the composition and number of tandem repeats among Bap proteins in the *A. baumannii* population are highly heterogeneous, and even the *bap* gene was found separated into different CDSs in some strains (De Gregorio et al. 2015). The latter was in fact the case for DSM30011, in which the *bap* gene was divided in two contiguous CDSs in a genomic locus that was conserved in other *A. baumannii* strains (supplementary table S12 and fig. S5, Supplementary Material online).

The *A. baumannii cpaA* gene encodes the metallopeptidase Cpa, an enzyme with the ability to cleave fibrinogen and deregulate blood coagulation (Tilley et al. 2014). CpaA, which was proposed to represent a virulence factor (Tilley et al. 2014), has been shown recently to represent a substrate of the Type II secretion system (Harding et al. 2016). Therefore, the conspicuous absence of *cpaA* in DSM30011 (table 4) and in the *A. baumannii* strains ATCC 17978 and ATCC 19606 isolated by the middle of last century (supplementary table S1, Supplementary Material online), supports proposals that this gene was recently acquired by *A. baumannii* in the clinical setting as the result of horizontal gene transfer events (Harding et al. 2016).

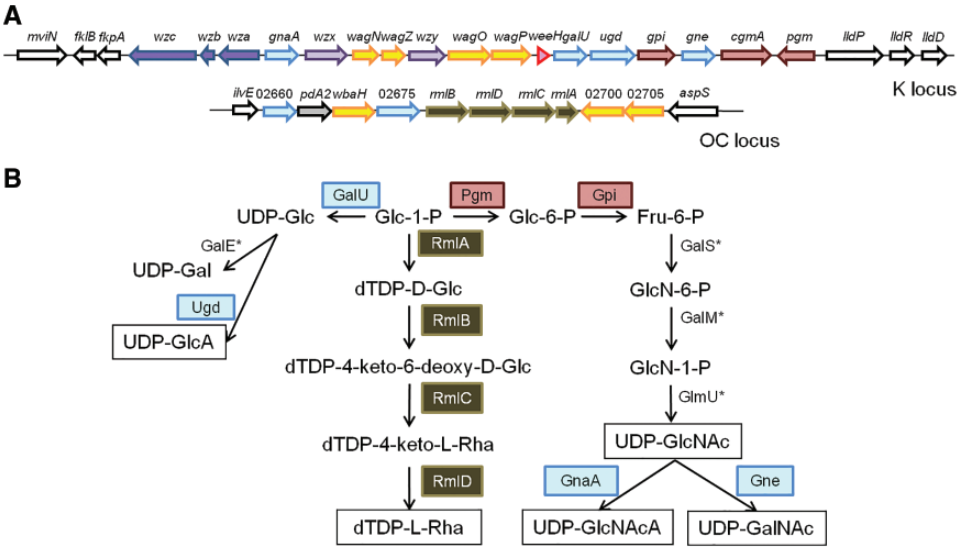

Fig. 4.—*A. baumannii* DSM30011 major polysaccharides. (*A*) Scheme showing the genetic organization of K and OC locus. Genes are colored according to the code used in supplementary table S12, Supplementary Material online. (*B*) Proposed biosynthetic pathways for sugars precursors of the main exopolysaccharides. Glc, D-glucose; GlcA, D-glucuronic acid; GlcN, 2-amino-2-deoxy-D-glucose; GlcNAc, 2-acetamido-2-deoxy-D-glucose; GlcNAcA, 2-acetamido-2-deoxy-D-glucuronic acid; Gal, D-galactose; GalA, D-galacturonic acid; GalNAc, 2-acetamido-2-deoxy-D-galactose. *The genes coding for these enzymes are located outside the K or OC gene clusters.

Conclusions

We traced in this work the origins of the *A. baumannii* DSM30011 collection strain to an isolate first reported in 1944 obtained from retting enrichment of the natural microbiota associated to a resin-producing desert shrub, guayule (Allen et al. 1944; Naghski et al. 1944). DSM30011 thus represents, to our knowledge, the earliest reported environmental *A. baumannii* strain isolated at the onset of the massive use of antibiotics starting by the middle of last century (Antunes et al. 2014). In concordance, DSM30011 showed general susceptibility to most clinically-employed antimicrobials including folate pathway inhibitors (table 3). Thus, this strain may certainly provide clues on the genomic content and diversity as well as niche ranges of the *A. baumannii* population that existed before the strong antimicrobial selection pressure associated to the antibiotic era (Antunes et al. 2014).

The genome analysis of DSM30011 revealed most of the traits that have been associated to *Acinetobacter* persistence and pathogenicity (Peleg et al. 2012; table 4 and supplementary table S12, Supplementary Material online). These include: 1) Two systems likely conferring the ability to endure in different environmental niches, such as a T6SS and associated gene clusters as well as a CRISPRs-cas system previously unreported in this species; 2) resistance genes against antimicrobials and other toxic compounds, including ADC-type AmpC and OXA-51-like β-lactamases and different efflux pumps; 3) systems driving genomic diversification such as different error-prone polymerases and Type IV pilus-mediated transformability; 4) genes encoding virulence mechanisms proposed for Acb clinical strains (table 4). On the contrary, DSM30011 lacks all RIs, ISs, GIs and plasmids typical of *Acinetobacter* clinical strains. This strongly suggests that these genetic elements of strong adaptive significance were recently acquired by infective *A. baumannii* lineages, most likely from other bacterial species co-existing in the clinical setting (Nigro and Hall 2011; Peleg et al. 2012; Antunes et al. 2014). This supports the notion that the highly selective conditions of the nosocomial environment have been crucial for both the adjustment of the expression of pathogenicity determinants and the acquisition of additional resistance traits that turned this species into a nosocomial pathogen (Antunes et al. 2014).

We also identified a previously unreported catabolic locus responsible of the complete degradation of acyclic monoterpenes, in addition to other catabolic pathways for many substances produced by plants including protective woody tissues (fig. 3*D*, supplementary tables S10 and S11, Supplementary Material online). The above features, added to the ability to endure high temperatures, are compatible with an organism thriving on resinous desert plants thus supporting such an environmental origin for DSM30011 (Allen et al. 1944). The presence of similar genomic features in all analyzed *A. baumannii* strains further suggests that resinous plants may provide environmental reservoirs for this species. In turn, it opens the possibility that certain phytophagous insects feeding in these plants (Morales-Jiménez et al. 2009; Keeling et al. 2013; Vilanova et al. 2014) represent vectors for the dissemination of *A. baumannii* in the environment.

Further studies on other *A. baumannii* strains of non-clinical origin are certainly required to elucidate the processes that led to the recent evolution of this species toward an opportunistic pathogen of humans.

Acknowledgments

We thank X. Charpentier (CIRI, Lyon, France) for the kind gift of the DSM30011 strain. We are indebted to J. Swezey (National Center for Agricultural Utilization Research, Agricultural Research Service, U.S. Department of Agriculture, Peoria, IL, USA) for providing us most valuable information concerning the NRRL collection strains B-551 and B-552. We are indebted to the curator teams of both the Institut Pasteur MLST system (Paris, France) and Oxford University (Oxford, UK) for their help in incorporating DSM30011 alleles and profiles at http://pubmlst.org/abaumannii/. We also thank P. Stothard for his generous help with the CGView software. This work was supported by a FINOVI Young Researcher Grant awarded to S.P.S.; by an Investissement d'Avenir (ANR-10-BINF-01-01) grant awarded to C.B.-A., and from grants to A.M.V. from the Agencia Nacional de Promoción Científica y Tecnológica (ANPCyT); Consejo Nacional de Investigaciones Científicas y Técnicas (CONICET-PIP1055); Ministerio de Ciencia, Tecnología e Innovación Productiva, Provincia de Santa Fe; Argentina. A.M.V., G.D.R., and M.E. are staff members of CONICET. C.B.-A. is member of the Institut Universitaire de France.

Supplementary Material

Supplementary data are available at *Genome Biology and Evolution* online.

Literature Cited

Allen PJ, Naghski J, Hoover SR. 1944. Decomposition of guayule resins by microorganisms. J Bacteriol. 47(6):559–572.

Altschul SF, et al. 1997. Gapped BLAST and PSI-BLAST: a new generation of protein database search programs. Nucleic Acids Res. 25:3389–3402.

Antunes LC, Imperi F, Towner KJ, Visca P. 2011. Genome-assisted identification of putative iron-utilization genes in *Acinetobacter baumannii* and their distribution among a genotypically diverse collection of clinical isolates. Res Microbiol. 162(3):279–284.

Antunes LCS, Visca P, Towner KJ. 2014. *Acinetobacter baumannii*: evolution of a global pathogen. Pathog Dis. 71(3):292–301.

Arndt D, et al. 2016. PHASTER: a better, faster version of the PHAST phage search tool. Nucleic Acids Res. 44(W1):W16–W21.

Aziz RK, et al. 2008. The RAST server: rapid annotations using subsystems technology. BMC Genomics. 9:75.

Baran W, Adamek E, Ziemiańska J, Sobczak A. 2011. Effects of the presence of sulfonamides in the environment and their influence on human health. J Hazard Mater. 196:1–15.

Barbe V, et al. 2004. Unique features revealed by the genome sequence of *Acinetobacter* sp. ADP1, a versatile and naturally transformation competent bacterium. Nucleic Acids Res. 32(19):5766–5779.

Bartual SG, et al. 2005. Development of a multilocus sequence typing scheme for characterization of clinical isolates of *Acinetobacter baumannii*. J Clin Microbiol. 43(9):4382–4390.

Bland C, et al. 2007. CRISPR Recognition Tool (CRT): a tool for automatic detection of clustered regularly interspaced palindromic repeats. BMC Bioinformatics. 8:209.

Bouvet PJM, Grimont PAD. 1986. Taxonomy of the genus *Acinetobacter* with the recognition of *Acinetobacter baumannii* sp. nov., *Acinetobacter haemolyticus* sp. nov., *Acinetobacter johnsonii* sp. nov., and *Acinetobacter junii* sp. nov. and emended descriptions of *Acinetobacter calcoaceticus* and *Acinetobacter lwoffii*. Int J Syst Bacteriol. 36(2):228–240.

Boyd E, Barkay T. 2012. The mercury resistance operon: from an origin in a geothermal environment to an efficient detoxification machine. Front Microbiol. 3:349.

Brown S, Amyes SG. 2005. The sequences of seven class D beta-lactamases isolated from carbapenem-resistant *Acinetobacter baumannii* from four continents. Clin Microbiol Infect. 11(4):326–329.

Clemmer KM, Bonomo RA, Rather PN. 2011. Genetic analysis of surface motility in *Acinetobacter baumannii*. Microbiology 157(Pt 9):2534–2544.

Criscuolo A, Gribaldo S. 2010. BMGE (Block Mapping and Gathering with Entropy): a new software for selection of phylogenetic informative regions from multiple sequence alignments. BMC Evol Biol. 10:210.

Darling AE, Mau B, Perna NT. 2010. ProgressiveMauve: multiple genome alignment with gene gain, loss and rearrangement. PLoS ONE. 5(6):e11147.

Davidov E, Kaufmann G. 2008. RloC: a wobble nucleotide-excising and zinc-responsive bacterial tRNase. Mol Microbiol. 69(6):1560–1574.

De Gregorio E, et al. 2015. Biofilm-associated proteins: news from *Acinetobacter*. BMC Genomics. 16:933.

Dhillon BK, et al. 2015. IslandViewer 3: more flexible, interactive genomic island discovery, visualization and analysis. Nucleic Acids Res. 43(W1):104–108.

Diancourt L, Passet V, Nemec A, Dijkshoorn L, Brisse S. 2010. The population structure of *Acinetobacter baumannii:* expanding multiresistant clones from an ancestral susceptible genetic pool. PLoS ONE. 5(4):e10034.

Di Nocera PP, Rocco F, Giannouli M, Triassi M, Zarrilli R. 2011. Genome organization of epidemic *Acinetobacter baumannii* strains. BMC Microbiol. 11:224.

Eijkelkamp BA, et al. 2011. Adherence and motility characteristics of clinical *Acinetobacter baumannii* isolates. FEMS Microbiol Lett. 323(1):44–51.

Eijkelkamp BA, Stroeher UH, Hassan KA, Paulsen IT, Brown MH. 2014. Comparative analysis of surface-exposed virulence factors of *Acinetobacter baumannii*. BMC Genomics. 15:1020.

Evans BA, Amyes SJ. 2014. OXA β-lactamases. Clin Microbiol Rev. 27(2):241–263.

Eveillard M, Kempf M, Belmonte O, Pailhoriès H, Joly-Guillou ML. 2013. Reservoirs of *Acinetobacter baumannii* outside the hospital and potential involvement in emerging human community-acquired infections. Int J Infect Dis. 17(10):e802–e805.

Farrugia DN, Elbourne LD, Mabbutt BC, Paulsen IT. 2015. A novel family of integrases associated with prophages and genomic islands integrated within the tRNA-dihydrouridine synthase A (*dusA*) gene. Nucleic Acids Res. 43(9):4547–4557.

Fiester SE, et al. 2016. Iron-regulated phospholipase c activity contributes to the cytolytic activity and virulence of *Acinetobacter baumannii*. PLoS ONE. 11(11):e0167068.

Förster-Fromme K, et al. 2006. Identification of genes and proteins necessary for catabolism of acyclic terpenes and leucine/isovalerate in *Pseudomonas aeruginosa*. Appl Environ Microbiol. 72(7):4819–4828.

Franceschi VR, Krokene P, Christiansen E, Krekling T. 2005. Anatomical and chemical defenses of conifer bark against bark beetles and other pests. New Phytol. 167(2):353–375.

Gao F, Zhang C-T. 2008. Ori-Finder: a web-based system for finding *oriC*s in unannotated bacterial genomes. BMC Bioinformatics. 9:79.

Graça J. 2015. Suberin: the biopolyester at the frontier of plants. Front Chem. 3:62.
Gerischer U, Ornston LN. 1995. Spontaneous mutations in pcaH and -G, structural genes for protocatechuate 3, 4-dioxygenase in *Acinetobacter calcoaceticus*. J Bacteriol. 177(5):1336–1347.
Gundi VA, Dijkshoorn L, Burignat S, Raoult D, La Scola B. 2009. Validation of partial *rpoB* gene sequence analysis for the identification of clinically important and emerging *Acinetobacter* species. Microbiology 155(Pt 7):2333–2341.
Hamidian M, Hall RM. 2016. *Acinetobacter baumannii* ATCC 19606 carries GIsul2 in a genomic island located in the chromosome. Antimicrob Agents Chemother. 61(1):e01991–16. pii: e01991-16.
Hamouda A, Evans BA, Towner KJ, Amyes SGB. 2010. Characterization of epidemiologically unrelated *Acinetobacter baumannii* isolates from four continents by use of multilocus sequence typing, pulsed-field gel electrophoresis, and sequence-based typing of blaOXA-51-like genes. J Clin Microbiol. 48(7):2476–2483.
Harding CM, et al. 2015. *Acinetobacter* strains carry two functional oligosaccharyltransferases, one devoted exclusively to type IV pilin, and the other one dedicated to O-glycosylation of multiple proteins. Mol Microbiol. 96(5):1023–1041.
Harding CM, Kinsella RL, Palmer LD, Skaar EP, Feldman MF. 2016. Medically relevant *Acinetobacter* species require a type II secretion system and specific membrane-associated chaperones for the export of multiple substrates and full virulence. PLoS Pathog. 12(1):e1005391.
Hare JM, Ferrell JC, Witkowski TA, Grice AN. 2014. Prophage induction and differential RecA and UmuDAb transcriptome regulation in the DNA damage responses of *Acinetobacter baumannii* and *Acinetobacter baylyi*. PLoS ONE. 9(4):e93861.
Heindorf M, Kadari M, Heider C, Skiebe E, Wilharm G. 2014. Impact of *Acinetobacter baumannii* superoxide dismutase on motility, virulence, oxidative stress resistance and susceptibility to antibiotics. PLoS ONE. 9(7):e101033.
Hu D, Liu B, Dijkshoorn L, Wang L, Reeves PR. 2013. Diversity in the major polysaccharide antigen of *Acinetobacter baumannii* assessed by DNA sequencing, and development of a molecular serotyping scheme. PLoS ONE. 8(7):e70329.
Jeon J, Kim J, Yong D, Lee K, Chong Y. 2012. Complete genome sequence of the podoviral bacteriophage YMC/09/02/B1251 ABA BP, which causes the lysis of an OXA-23 producing carbapenem-resistant *Acinetobacter baumannii* isolate from a septic patient. J Virol. 86(22):12437–12438.
Jolley KA, Maiden MC. 2010. BIGSdb: Scalable analysis of bacterial genome variation at the population level. BMC Bioinformatics. 11(1):595.
Karah N, Sundsfjord A, Towner K, Samuelsen Ø. 2012. Insights into the global molecular epidemiology of carbapenem non-susceptible clones of *Acinetobacter baumannii*. Drug Resist Update. 15(4):237–247.
Karah N, et al. 2015. CRISPR-*cas* subtype I-Fb in *Acinetobacter baumannii*: evolution and utilization for strain subtyping. PLoS ONE. 10(2):e0118205.
Keeling CI, et al. 2013. Draft genome of the mountain pine beetle, *Dendroctonus ponderosae* Hopkins, a major forest pest. Genome Biol. 14:R27.
Koenigs A, Zipfel PF, Kraiczy P. 2015. Translation elongation factor Tuf of *Acinetobacter baumannii* is a plasminogen-binding protein. PLoS ONE. 10(7):e0134418.
Koenigs A, et al. 2016. CipA of *Acinetobacter baumannii* is a novel plasminogen binding and complement inhibitory protein. J Infect Dis. 213:1388–1399.
La Scola B, Gundi VA, Khamis A, Raoult D. 2006. Sequencing of the *rpoB* gene and flanking spacers for molecular identification of *Acinetobacter* species. J Clin Microbiol. 44(3):827–832.
Limansky AS, Viale AM. 2002. Can composition and structural features of oligonucleotides contribute to their wide-scale applicability as random PCR primers in mapping bacterial genome diversity? J Microbiol Methods. 50(3):291–297.
Loewen PC, Alsaadi Y, Fernando D, Kumar A. 2014. Genome sequence of a tigecycline-resistant clinical isolate of *Acinetobacter baumannii* strain AB031 obtained from a bloodstream infection. Genome Announc. 2(5):e01036–14.
Longo F, Vuotto C, Donelli G. 2014. Biofilm formation in *Acinetobacter baumannii*. New Microbiol. 37(2):119–127.
Makarova KS, Wolf YI, Snir S, Koonin EV. 2011. Defense islands in bacterial and archaeal genomes and prediction of novel defense systems. J Bacteriol. 193(21):6039–6056.
Makarova KS, Koonin EV. 2015. Annotation and classification of CRISPR-Cas Systems. In: Lundgren M, Charpentier E, Fineran PC, editors. CRISPR. Methods and protocols. Vol. 1311. New York: Springer. pp. 47–75. ISBN 978-1-4939-2686-2.
Miele V, Penel S, Duret L. 2011. Ultra-fast sequence clustering from similarity networks with SiLiX. BMC Bioinformatics. 12:116.
Morales-Jiménez J, Zúñiga G, Villa-Tanaca L, Hernández-Rodríguez C. 2009. Bacterial community and nitrogen fixation in the red turpentine beetle, *Dendroctonus valens* LeConte (Coleoptera: Curculionidae: Scolytinae). Microb Ecol. 58(4):879–891.
Morán-Barrio J, et al. 2017. The *Acinetobacter* outer membrane contains multiple specific channels for carbapenem β-lactams as revealed by kinetic characterization analyses of imipenem permeation into *Acinetobacter baylyi* cells. Antimicrob Agents Chemother. 61(3):e01737–16.
Mortensen BL, Skaar EP. 2013. The contribution of nutrient metal acquisition and metabolism to *Acinetobacter baumannii* survival within the host. Front Cell Infect Microbiol. 3:95.
Mussi MA, et al. 2011. Horizontal gene transfer and assortative recombination within the *Acinetobacter baumannii* clinical population provide genetic diversity at the single *carO* gene, encoding a major outer membrane protein channel. J Bacteriol. 193(18):4736–4648.
Naghski J, White JW, Hoover SR. 1944. Aerobic decomposition of Guayule Shrub (*Parthenium argentatum* Gray). J Bacteriol. 48(2):159–178.
Nait Chabane Y, et al. 2014. Characterisation of pellicles formed by *Acinetobacter baumannii* at the air–liquid interface. PLoS ONE. 9(10):e111660.
Nemec A, et al. 2011. Genotypic and phenotypic characterization of the *Acinetobacter calcoaceticus–Acinetobacter baumannii* complex with the proposal of *Acinetobacter pittii* sp. nov. (formerly *Acinetobacter* genomic species 3) and *Acinetobacter nosocomialis* sp. nov. (formerly *Acinetobacter* genomic species 13TU). Res Microbiol. 162(4):393–404.
Nguyen LT, Schmidt HA, von Haeseler A, Minh BQ. 2015. IQ-TREE: a fast and effective stochastic algorithm for estimating maximum-likelihood phylogenies. Mol Biol Evol. 32(1):268–274.
Nigro SJ, Hall RM. 2011. GI*sul2*, a genomic island carrying the *sul2* sulphonamide resistance gene and the small mobile element CR2 found in the *Enterobacter cloacae* subspecies *cloacae* type strain ATCC 13047 from 1890, *Shigella flexneri* ATCC 700930 from 1954 and *Acinetobacter baumannii* ATCC 17978 from 1951. J Antimicrob Chemother. 66(9):2175–2176.
Nigro SJ, Post V, Hall RM. 2011. Aminoglycoside resistance in multiply antibiotic-resistant *Acinetobacter baumannii* belonging to global clone 2 from Australian hospitals. J Antimicrob Chemother. 66(7):1504–1509.
Norton MD, Spilkia AJ, Godoy VG. 2013. Antibiotic resistance acquired through a DNA damage-inducible response in *Acinetobacter baumannii*. J Bacteriol. 195(6):1335–1345.
Peleg AY, et al. 2012. The success of *Acinetobacter* species; genetic, metabolic and virulence attributes. PLoS ONE. 7(10):e46984.
Post V, White PA, Hall RM. 2010. Evolution of AbaR-type genomic resistance islands in multiply antibiotic-resistant *Acinetobacter baumannii*. J Antimicrob Chemother. 65(6):1162–1170.

Ravasi P, Limansky AS, Rodriguez RE, Viale AM, Mussi MA. 2011. ISAba825, a functional insertion sequence modulating genomic plasticity and bla(OXA-58) expression in *Acinetobacter baumannii*. Antimicrob Agents Chemother. 55(2):917–920.

Repizo GD, et al. 2014. Genomic comparative analysis of the environmental *Enterococcus mundtii* against enterococcal representative species. BMC Genomics. 15(1):489.

Repizo GD, et al. 2015. Differential role of the T6SS in *Acinetobacter baumannii* virulence. PLoS ONE. 10(9):e0138265.

Roca I, Espinal P, Vila-Farrés X, Vila J. 2012. The *Acinetobacter baumannii* oxymoron: commensal hospital dweller turned pan-drug-resistant menace. Front Microbiol. 3:148.

Russo T, et al. 2010. The K1 capsular polysaccharide of *Acinetobacter baumannii* strain 307-0294 is a major virulence factor. Infect Immun. 78(9):3993.

Siguier P, Perochon J, Lestrade L, Mahillon J, Chandler M. 2006. ISfinder: the reference centre for bacterial insertion sequences. Nucleic Acids Res. 34(90001):D32–D36.

Skiebe E, et al. 2012. Surface-associated motility, a common trait of clinical isolates of *Acinetobacter baumannii*, depends on 1, 3-diaminopropane. Int J Med Microbiol. 302(3):117–128.

Smith MA, Weaver VB, Young DM, Ornston LN. 2003. Genes for chlorogenate and hydroxycinnamate catabolism (hca) are linked to functionally related genes in the dca-pca-qui-pob-hca chromosomal cluster of *Acinetobacter* sp. strain ADP1. Appl Environ Microbiol. 69(1):524–532.

Stahl J, Bergmann H, Göttig S, Ebersberger I, Averhoff B. 2015. *Acinetobacter baumannii* virulence is mediated by the concerted action of three phospholipases D. PLoS ONE. 10(9):e0138360.

Stothard P, Wishart DS. 2005. Circular genome visualization and exploration using CGView. Bioinformatics. 21(4):537–539.

Tada T, Miyoshi-Akiyama T, Shimada K, Shimojima M, Kirikae T. 2014. Dissemination of 16S rRNA methylase armA-producing *Acinetobacter baumannii* and emergence of OXA-72 carbapenemase coproducers in Japan. Antimicrob Agents Chemother. 58(5):2916–2920.

Thornley MJ. 1967. A taxonomic study of *Acinetobacter* and related genera. J Gen Microbiol. 49(2):211–257.

Tilley D, Law R, Warren S, Samis JA, Kumar A. 2014. CpaA a novel protease from *Acinetobacter baumannii* clinical isolates deregulates blood coagulation. FEMS Microbiol Lett. 356(1):53–61. Epub 2014/06/10.

Touchon M, et al. 2014. The genomic diversification of the whole *Acinetobacter* genus: origins, mechanisms, and consequences. Genome Biol Evol. 6(10):2866–2882.

Turton JF, et al. 2006. Identification of *Acinetobacter baumannii* by detection of the blaOXA-51-like carbapenemase gene intrinsic to this species. J Clin Microbiol. 44(8):2974–2976.

Vallenet D, et al. 2008. Comparative analysis of *Acinetobacters*: three genomes for three lifestyles. PLoS ONE. 3(3):e1805.

Varani AM, Siguier P, Gourbeyre E, Charneau V, Chandler M. 2011. ISsaga is an ensemble of web-based methods for high throughput identification and semi-automatic annotation of insertion sequences in prokaryotic genomes. Genome Biol. 12(3):R30.

Vilanova C, Marín M, Baixeras J, Latorre A, Porcar M. 2014. Selecting microbial strains from pine tree resin: biotechnological applications from a terpene world. PLoS ONE. 9(6):e100740.

Wilharm G, Piesker J, Laue M, Skiebe E. 2013. DNA Uptake by the nosocomial pathogen *Acinetobacter baumannii* occurs during movement along wet surfaces. J Bacteriol. 195(18):4146–4153.

Zankari E, et al. 2012. Identification of acquired antimicrobial resistance genes. J Antimicrob Chemother. 67(11):2640–2644.

Zhou Y, Liang Y, Lynch KH, Dennis JJ, Wishart DS. 2011. PHAST: a fast phage search tool. Nucleic Acids Res. 39(Web Server issue):W347–W352.

Zulak KG, Bohlmann J. 2010. Terpenoid biosynthesis and specialized vascular cells of conifer defense. J Integr Plant Biol. 52(1):86–97.

Associate editor: Esperanza Martinez-Romero